Sensors and Actuators B 255 (2018) 3093–3101

Contents lists available at ScienceDirect

Sensors and Actuators B: Chemical

journal homepage: www.elsevier.com/locate/snb

A colorimetric sensor based on citrate-stabilized AuNPs for rapid pesticide residue detection of terbuthylazine and dimethoate

Ningyi Chen[a,b,1], Hongyu Liu[a,b,1], Yujie Zhang[a], Zhuangwei Zhou[a], Wenpei Fan[c], Guocan Yu[c], Zheyu Shen[a,c,**], Aiguo Wu[a,*]

[a] CAS Key Laboratory of Magnetic Materials and Devices & Division of Functional Materials and Nanodevices, Ningbo Institute of Materials Technology and Engineering, Chinese Academy of Sciences, Ningbo, Zhejiang 315201, China
[b] Nano Science and Technology Institute, University of Science and Technology of China, Suzhou, Jiangsu 215123, China
[c] Laboratory of Molecular Imaging and Nanomedicine (LOMIN), National Institute of Biomedical Imaging and Bioengineering (NIBIB), National Institutes of Health (NIH), Bethesda, MD 20892, United States

ARTICLE INFO

Article history:
Received 20 May 2017
Received in revised form
15 September 2017
Accepted 20 September 2017
Available online 28 September 2017

Keywords:
Colorimetric sensor
Citrate-stabilized AuNPs
Rapid pesticide residue detection
Terbuthylazine
Dimethoate

ABSTRACT

A new colorimetric sensor based on citrate-stabilized AuNPs was proposed for the rapid pesticide residue detection of both terbuthylazine (TBA) and dimethoate (DMT) with ultra-sensitivities and high selectivities. The detection mechanisms have been verified via FT-IR, UV–vis spectra, Zeta Potential, TEM and DLS. Under the optimized experimental conditions, 30 kinds of potential environmental pollutants have no interference on the TBA or DMT detection indicating the high selectivities of our AuNP-based colorimetric sensor. The limit of detections (LODs) of TBA and DMT by eye vision are respectively 0.3 μM and 20 nM, and those based on calculation (3σ/S) are 0.02 μM and 6.2 nM, respectively. The minimum detectable concentrations of TBA or DMT are much lower than the maximum residue limit (MRL) regulated by the governments of EU and China. The linear relationships of the UV–vis spectrometry demonstrate that our AuNP-based colorimetric sensor can be used for the quantitative analysis of TBA in the range of 0.1–0.9 μM, and DMT in the range of 1–40 nM. Finally, our AuNP-based colorimetric sensor is also verified to have a good practical applicability for TBA or DMT detection in the real environmental samples.

1. Introduction

In the process of agricultural production, herbicides and insecticides are two special agricultural chemicals, and have been widely used to ensure the harvest [1–3]. Terbuthylazine (TBA) is a widely used pre- and post- bud herbicide, which is mainly used for the removal of broad-leaved weeds and annual weeds [4,5]. Dimethoate (DMT) is a member of the most common organic phosphorus insecticides (i.e. a group of broad-spectrum insecticidal agents). The DMT is widely used for treatment of plant diseases and insect pests [6,7]. However, TBA and DMT are the primary source of environmental pollution and food toxicity. They bring some negative effects to the safety and health of the people, and the situation continues to deteriorate [8,9]. In 2015, the European Union (EU) listed 74 pesticides (including the TBA and DMT) that have chronic toxicity to humans. The maximum residue limits (MRL) of TBA and DMT in water or food have been respectively regulated to 0.05 mg/kg and 0.02 mg/kg (i.e. 0.22 μM for TBA and 87 nM for DMT) by the governments of EU and China (GB2763-2014) [10–12].

To ensure the food safety and protect the health of consumers, there have been lots of efforts to develop various strategies for the detection and quantification of TBA and DMT in environmental samples, such as gas chromatography (GC) [13–15], high performance liquid chromatography (HPLC) [16,17], fluorescence spectrometry [18,19] and other related technologies [20–22]. Although these methods have high sensitivity, many of them are complicated and time-consuming, require bulky instrumentation, and have to be performed by highly trained technicians. Moreover, these big instruments cannot be used on site for detection of real environmental samples.

Recently, noble metal-based nanomaterials have emerged as powerful tools for simple and rapid pesticide residue detection

* Corresponding author.
** Corresponding author at: CAS Key Laboratory of Magnetic Materials and Devices & Division of Functional Materials and Nanodevices, Ningbo Institute of Materials Technology and Engineering, Chinese Academy of Sciences, Ningbo, Zhejiang 315201, China.
E-mail addresses: shenzheyu@nimte.ac.cn (Z. Shen), aiguo@nimte.ac.cn (A. Wu).
[1] Both authors contributed equally to this work.

https://doi.org/10.1016/j.snb.2017.09.134
0925-4005/

with high sensitivity and specificity, such as quinalphos insecticide, malathion and glyphosate [23–25]. However, there is little research reported on rapid pesticide residue detection of DMT based on the noble metal-based nanomaterials. Lang et al. developed a sensitive amperometric acetylcholinesterase biosensor based on gold nanorods (AuNRs) for the detection of DMT. This method is highly sensitive and the limit of detection (LOD) is 3.9 nM. However, the synthesis of the biosensor is cumbersome and the storage requires a high criterion (in dark and dry place at 0 °C) [26]. Dar et al. explored a colorimetric chemo-sensor based on gold nanoparticles (AuNPs), and obtained a linear relationship between the fluorescence intensity and DMT concentration, which could be used for the quantitative analysis of DMT. The LOD is 16.4 μM. But this method is based on fluorescence spectrometry, and cannot be used for on-site detection of real environmental samples [27]. Lodha's group proposed a facile strategy for preparing highly stable *p*-sulphonatocalix resorcinarene modified silver nanoprobe in aqueous media for DMT detection. Although the sensitivity is high with the LOD of 80 nM, only 6 kinds of pesticides were used as the interfering substances to clarify the specificity [28].

In addition, to the best of our knowledge, noble metal-based colorimetric nanosensor has not yet been reported for the rapid pesticide residue detection of TBA. Furthermore, it is rarely reported that one noble metal-based nanosensor could be used for colorimetric detection of two environmental pollutants.

In this study, we developed a new colorimetric sensor based on citrate-stabilized AuNPs, which could be used for the rapid pesticide residue detection of both TBA and DMT with ultra-sensitivities and high selectivities. The schematic illustration is shown in Scheme 1.

The TBA detection is based on an aggregation mechanism (Scheme 1a). NaOH only play a role in regulating the pH of the detection solution for better recognition of TBA. Moreover, citrate-stabilized AuNP dispersions are stable incubated with NaOH (20 μL, 1.0 M). After addition of a mixture of NaOH (20 μL, 1.0 M) and TBA (100 μL, >0.02 μM) into our AuNP-based colorimetric sensor (0.88 mL, C_{Au} = 0.25 mM), the ionic interaction between the strong positive charge of TBA and negative charge of citrate on the surface of AuNPs results in the AuNPs' aggregation. However, the AuNPs of the colorimetric sensor are well-dispersed after addition of the same amount of NaOH without TBA, which are used as the control for the TBA detection. The aggregation of AuNPs leads to obvious red shift of the UV–vis spectrum and clear color change of the colorimetric sensor from red to blue. Based on this aggregation mechanism, the pesticide residue of TBA could be rapidly detected by visualizing the color change of the sensor or measuring the UV–vis spectrum. Our AuNP-based sensor has an ultra-sensitivity and a high selectivity for the TBA detection because the extinction coefficient of AuNPs is high and the positive charge of TBA is very strong compared with other pesticides and normal substances in real environmental samples.

On the contrary, the DMT detection is built on an anti-aggregation mechanism (Scheme 1a). Because DMT belongs to acid pesticide that is easily hydrolyzed in a strong alkaline environment, NaOH is used to hydrolyze the DMT to realize the detection. After mixing of NaOH (40 μL, 1.0 M) and DMT (100 μL, >6.2 nM), the DMT is hydrolyzed quickly and the hydrolysis product is negatively charged (Scheme 1b). Therefore, after addition of a mixture of NaOH and DMT into our AuNP-based colorimetric sensor (0.88 mL, C_{Au} = 0.25 mM), the AuNPs of the colorimetric sensor are well-dispersed under stabilization of the DMT hydrolysis product with strong negative charges. In addition, the AuNPs of the colorimetric sensor are aggregated after addition of same amount of NaOH without DMT due to the high ionic strength, which are used as the control for the DMT detection. The anti-aggregation of AuNPs leads to obvious blue shift of the UV–vis spectrum and clear color change of the colorimetric sensor from grey to red. Based on this anti-aggregation mechanism, the pesticide residue of DMT can also be rapidly detected by visualizing the color change of the sensor or measuring the UV–vis spectrum. Our AuNP-based sensor also has an ultra-sensitivity and a high selectivity for the DMT detection because of the high extinction coefficient of AuNPs and the specific reaction of DMT at strong alkaline conditions.

The applicability of our AuNP-based colorimetric sensor is also verified by detection of TBA and DMT in real environmental samples.

2. Experimental

2.1. Materials and instrumentation

Gold(III) chloride trihydrate ($HAuCl_4{\cdot}3H_2O$), sodium citrate dihydrate ($Na_3Ct{\cdot}2H_2O$), HCl, HNO_3 and NaOH were obtained from Sinopharm Chemical Reagent Co. Ltd (Shanghai, China). Atrazine and glyphosate were obtained from J&K Scientific Ltd. (Beijing, China). Melamine iprodione, dipterex, regent, indoxacarb, fenobucarb, pretilachlor, isoprocarb, pymetrozine were purchased from Aladdin-Reagent Co.,Ltd. (Shanghai, China). MCPA-Na was obtained from Sigma-Aldrich (Shanghai, China). Chemicals of analytical reagent grade were used without further purification and all solutions were prepared with Milli-Q water.

Transmission electron microscopy (TEM) images were obtained on a JEOL 2100 microscope operated at 200 kV. Dynamic light scattering (DLS) and Zeta potential measurements were made on a Zetasizer instrumentation (Nano ZS, Malvern Instruments Ltd). Fourier transform infrared (FT-IR) spectroscopy was recorded on a Nicolet 6700 spectrophotometer (Thermo Scientific, USA). UV–vis spectra were obtained on an ultraviolet and visible spectrophotometer (T10CS, PERSEE, China).

2.2. Preparation of the citrate-stabilized AuNPs

The citrate-stabilized AuNPs with an average diameter of 16 nm were prepared according to previously published protocols [29–31]. Typically, 5.0 mL of $HAuCl_4$ aqueous solution (5.0 mM) was added to 92.5 mL of Milli-Q water in a round-bottom flask. The solution was then heated to be boiling under vigorous magnetic stirring. After that, 2.0 mL of Na_3Ct solution (10 mg/mL) was charged, which results in a solution color change from pale yellow to deep red. After this color change, the heating was stopped immediately. The obtained AuNP dispersion was cooled down at room temperature and kept in the refrigerator (4 °C) until use.

2.3. Rapid colorimetric detection of TBA and DMT

For the rapid colorimetric detection of TBA, 100 μL of TBA aqueous solutions with various concentrations (0.1 5.0 μM) were first mixed with various volume of NaOH (1.0 M). The mixture was then added into the above obtained AuNP-based colorimetric sensor (0.88 mL, C_{Au} = 0.25 mM). The mixtures were kept at room temperature for 1.0 30 min before the colorimetry observation or spectrometry measurement. Addition of the same amount of NaOH without TBA into the AuNP-based sensor was used as the control of TBA detection.

For rapid colorimetric detection of DMT, 100 μL of DMT aqueous solutions with different concentrations (1 5000 nM) were first mixed with different volume of NaOH (1.0 M). Then, the mixture was added into the AuNP-based colorimetric sensor (0.86 mL, C_{Au} = 0.25 mM). The mixtures were kept at room temperature for 1.0 30 min before the colorimetry observation or spectrometry detection. Addition of the same amount of NaOH

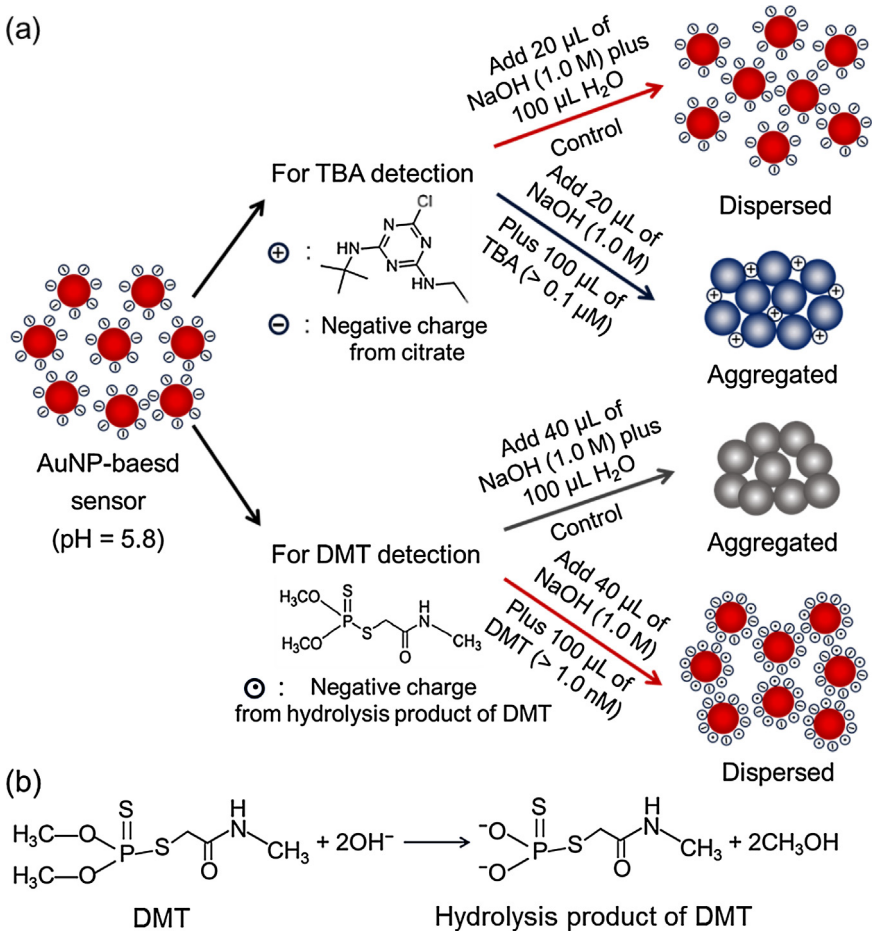

Scheme 1. (a): Schematic illustration of the mechanisms of the AuNP-based colorimetric sensor for rapid pesticide residue detection of terbuthylazine (TBA) and dimethoate (DMT); (b): Reaction equation of the DMT at alkaline conditions.

without DMT into the AuNP-based sensor was used as the control of DMT detection.

2.4. Detection of real environmental samples

Our AuNP-based colorimetric sensor was also applied for the rapid detection of TBA or DMT in real environmental samples including the tap water (collected through our institutional facility), green tea and apple juice. These samples were first filtered using syringe filters with 0.22 μm of membrane to remove the insoluble substance. Standard solutions of TBA (0.1 2.5 μM) or DMT (10 500 nM) were then added into the purified real environmental samples. After that, the TBA and DMT in these samples were detected using the AuNP-based colorimetric sensor based on the above protocols.

3. Results and discussion

3.1. Detection mechanism of TBA by the AuNP-based colorimetric sensor

The detection mechanism of TBA by our AuNP-based colorimetric sensor as shown in Scheme 1 was verified via FT-IR, UV–vis spectra, Zeta Potential, TEM and DLS.

The AuNP-based colorimetric sensor (i.e. citrate-stabilized AuNPs) was synthesized by the reduction of $HAuCl_4$ with sodium citrate. During the synthesis process, the sodium citrate can also be capped onto the surface of the AuNPs, which is verified by the negative Zeta potential (-34.4 mV, Table S1).

In the FT-IR spectra of our AuNP-based colorimetric sensor incubated with NaOH (control) or NaOH plus TBA (Fig. S1), the strong peak at 1731 cm^{-1} confirms the presence of —COOH groups, which further indicates that the sodium citrate encircles the AuNPs as a stabilizer. In addition, the TBA is a typical triazine herbicide and contains lots of amino groups, which is easy to generate positive charges [32–34]. The strong peaks at 1613 cm^{-1} and 1585 cm^{-1} respectively confirm the presence of C=N and NH groups of TBA in the sample of AuNP-based colorimetric sensor incubated with NaOH plus TBA. This result demonstrates that the TBA is absorbed onto the surface of AuNPs because the samples are washed using Milli-Q water before FT-IR measurements.

Fig. 1a shows the photographic image and UV–vis spectra of the citrate-stabilized AuNP dispersions (0.88 mL, C_{Au} = 0.25 mM) incubated with 20 μL of NaOH (1.0 M) plus 100 μL of H_2O (control), or with 20 μL of NaOH (1.0 M) plus 100 μL of TBA (1.0 μM). It is found that the AuNP dispersion of the control is wine red and its UV–vis spectrum has a specific peak at 520 nm, which indicates that the AuNPs of the control sample are stable. That's because the electrostatic repulsion is strong at −35.3 mV of Zeta potential (Table S1). However, after incubation with the mixture of NaOH (20 μL, 1.0 M) and TBA (100 μL, 1.0 μM) for 5.0 min, the color of the AuNP dispersion changes from red to blue. In addition, the UV–vis absorption peak at 520 nm decreases and a new absorption peak at 650 nm emerges. These results suggest that the TBA leads to aggregation of

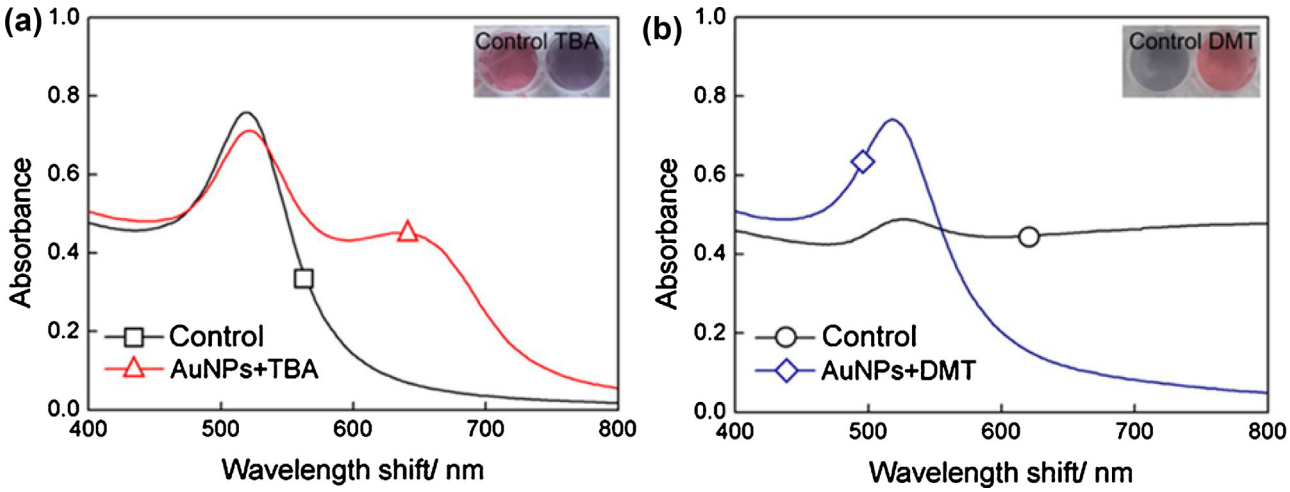

Fig. 1. (a): Photographic image and UV–vis spectra of the citrate-stabilized AuNP dispersions (0.88 mL, C_{Au} = 0.25 mM) incubated with 20 μL of NaOH (1.0 M) plus 100 μL of H_2O (control), or with 20 μL of NaOH (1.0 M) plus 100 μL of TBA (1.0 μM); (b): Photographic image and UV–vis spectra of AuNP dispersions (0.86 mL, C_{Au} = 0.25 mM) incubated with 40 μL of NaOH (1.0 M) plus 100 μL of H_2O (control), or with 40 μL of NaOH (1.0 M) plus 100 μL of DMT (0.2 μM).

the AuNPs via decreasing the electrostatic repulsion, which is weak at 5.4 mV of Zeta potential (Table S1).

This aggregation mechanism for TBA detection is further verified by TEM images (Fig. 2a and b) and DLS size distributions (Fig. S3a). We can see the AuNPs of the control sample are well dispersed and the hydrodynamic size is ~16 nm. However, the AuNPs after incubation with the mixture of NaOH (20 μL, 1.0 M) and TBA (100 μL, 1.0 μM) aggregate significantly and the hydrodynamic size increases to ~172 nm.

3.2. Detection mechanism of DMT by the AuNP-based colorimetric sensor

The detection mechanism of DMT by our AuNP-based colorimetric sensor as shown in Scheme 1 was also verified via FT-IR, UV–vis spectra, Zeta Potential, TEM and DLS.

Fig. S2 shows the FT-IR spectra of the citrate-stabilized AuNPs (0.86 mL, C_{Au} = 0.25 mM) incubated with 40 μL of NaOH (1.0 M) plus 100 μL of H_2O (control) or incubated with a mixture of NaOH (40 μL, 1.0 M) and DMT (100 μL, 10 μM). Most of functional groups including —COOH are not observable for the control sample (Fig. S2a) due to the serious aggregation of the AuNPs. In addition, it was reported that the DMT can be hydrolyzed at strong alkali conditions resulting from breakage of P—O—C group [35–37]. The hydrolysis reaction is illustrated in Scheme 1b. The emerging of a peak at 2107 cm^{-1} (i.e. C—O···H group) in our FT-IR spectrum (Fig. S2b) confirms this reaction.

Fig. 1b shows the corresponding photographic image and UV–vis spectra of the AuNPs (0.86 mL, C_{Au} = 0.25 mM) incubated with 40 μL of NaOH (1.0 M) plus 100 μL of H_2O (control) or incubated with a mixture of NaOH (40 μL, 1.0 M) and DMT (100 μL, 0.2 μM). It can be seen that the color of the control sample is grey and the UV–vis spectrum at visible region is dampened because the AuNPs aggregated severely due to the low electrostatic repulsion at high ionic strength (Zeta potential ≃3.3 mV, Table S1). However, after incubation of the mixture of NaOH and DMT, the AuNP dispersion color remains red and the UV–vis spectrum at 525 nm exhibited an obvious absorption peak. That's because the hydrolysis product of DMT absorbed the surface of AuNPs significantly increase the electrostatic repulsion (Zeta potential ≃35.8 mV, Table S1) resulting anti-aggregation of the AuNPs.

This anti-aggregation mechanism for DMT detection is further verified by TEM images (Fig. 2c and d) and DLS size distributions (Fig. S3b). It is found that the AuNPs of the control sample aggregate severely and the hydrodynamic size is ~246 nm. However, the AuNPs after incubation with the mixture of NaOH (40 μL, 1.0 M) and DMT (100 μL, 0.2 μM) are well dispersed and the hydrodynamic size is around 16 nm.

3.3. Optimization of experimental conditions

Based on the above-verified two mechanisms, our AuNP-based colorimetric sensor is promising for rapid pesticide residue detection of both TBA and DMT. The system color changes immediately when the detection object (TBA or DMT) is added to the system. But the detection sensitivities and specificities of the AuNPs-based colorimetric probe could be greatly influenced by the process of aggregation or anti-aggregation. In order to enhance that, we optimized the experimental conditions for TBA and DMT detection including the volume of NaOH (1.0 M) and the incubation time of AuNPs with TBA or DMT according to the sensing effect.

As shown in Fig. S4a, when the volume of NaOH (1.0 M) is in the range of 10 28 μL, the color of the control sample is red. However, the color changes to grey when the NaOH volume is increased to 36 μL. This result indicates that the AuNPs are unstable and become aggregated at the high amount of NaOH. In addition, when the volume of NaOH ranges from 10 to 28 μL, the color of our AuNP-based sensors with the addition of NaOH and TBA gradually changes from purple or blue. The colorimetric sensing effect seems to be best when the NaOH volume is 20 μL, which is also confirmed by the UV–vis absorption plot of A/A_0 (A_0 represents the UV–vis absorbance of the AuNP-based sensor at 650 nm in the control group, and A is the absorbance of the AuNP-based sensor at 650 nm after addition of TBA). Therefore, the volume of NaOH (1.0 M) is optimized to be 20 μL for detection of TBA using our AuNP-based sensor.

Fig. S4b shows the influence of the incubation time (after addition of NaOH and TBA into the AuNP-based sensor) on the detection effect of TBA using our AuNP-based sensor. It is found that the A/A_0 is almost maximum at 5.0 min of incubation time, which indicates that 5.0 min is enough to reach the reaction equilibrium. Therefore, to obtain the maximum response to TBA, 5.0 min is chosen as an optimal incubation time for the following experiments.

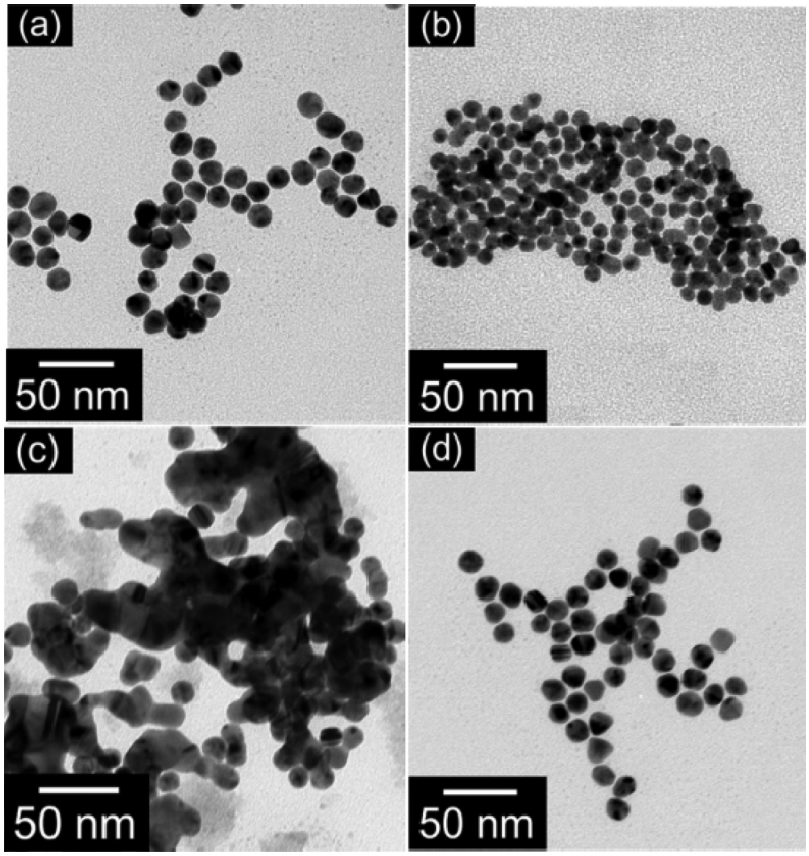

Fig. 2. TEM images of the citrate-stabilized AuNPs at different conditions. (a): AuNPs (0.88 mL, C_{Au} = 0.25 mM) incubated (5 min) with 20 μL of NaOH (1.0 M) plus 100 μL of H_2O (control); (b): AuNPs (0.88 mL, C_{Au} = 0.25 mM) incubated with 20 μL of NaOH (1.0 M) plus 100 μL of TBA (1.0 μM); (c): AuNPs (0.86 mL, C_{Au} = 0.25 mM) incubated (10 min) with 40 μL of NaOH (1.0 M) plus 100 μL of H_2O (control); (d): AuNPs (0.86 mL, C_{Au} = 0.25 mM) incubated with 40 μL of NaOH (1.0 M) plus 100 μL of DMT (0.2 μM).

Subsequently, the influence of the NaOH (1.0 M) volume and incubation time (after addition of NaOH and DMT into the AuNP-based sensor) on the detection effect of DMT using our AuNP-based sensor was further investigated (Fig. S5). When the volume of NaOH (1.0 M) is 20 μL, the color of the control sample is red. However, the color changes to grey when the NaOH volume is in the range 30 60 μL (Fig. S5a). This result indicates that NaOH volume should be higher than 30 μL for DMT detection based on the anti-aggregation mechanism. In addition, when the volume of NaOH ranges from 30 60 μL, the color of our AuNP-based sensors with the addition of NaOH and DMT is red, and gradually changes to darker. The colorimetric sensing effect looks like best when the NaOH volume is 40 μL, which is further confirmed by the UV–vis absorption plot of A/A_0 (A_0 represents the UV–vis absorbance of the AuNP-based sensor at 525 nm in the control group, and A is the absorbance of the AuNP-based sensor at 525 nm after addition of DMT). Therefore, the volume of NaOH (1.0 M) is optimized to be 40 μL for detection of DMT using our AuNP-based sensor.

Fig. S5b shows the influence of the incubation time (after addition of NaOH and DMT into the AuNP-based sensor) on the detection effect of DMT using our AuNP-based sensor. We can see the A/A_0 is almost maximum at 10 min of incubation time because 10 min is enough to achieve the reaction equilibrium. Therefore, to obtain the maximum response to DMT, 10 min is chosen as one of the optimized conditions for the subsequent studies.

3.4. Specificity of the AuNP-based colorimetric sensor for TBA or DMT

The specificity of our AuNP-based colorimetric sensor was evaluated for TBA or DMT compared with 30 kinds of potential environmental pollutants including other pesticides or ions, such as iprodione, dioxacarb, benzex, isoprocarb, chipton, pretilachlor, sodium cyclamate, permethrin, trichlorphon, fenvalerate, chlorpyrifos, profenofos, indoxacarb, dichlorodiphenyltrichloroethane, glufosinate-ammonium, glyphosate, deltamethrin, D-glucose, aspartame, K^+, Na^+, Mg^{2+}, Ba^{2+}, Cl^-, NO_3^-, Ac^-, CO_3^{2-}, SO_4^{2-} and PO_4^{3-}. As shown in Fig. 3a, TBA can result in an obvious red shift of the UV–vis absorption spectrum compared with the control. However, other environmental pollutants have an influence on the UV–vis absorption spectrum. In addition, color of the sensors incubated with the environmental pollutants are all red, and similar to that of the control. But that of the sensor incubated with TBA is blue (Fig. 3b). These results demonstrate that these potential environmental pollutants have no interference to TBA detection using our AuNP-based colorimetric sensor.

Fig. 3c and Fig. 3d respectively show the UV–vis absorption spectra and photographic images of the AuNP-based colorimetric sensor (0.86 mL) incubated (10 min) with 40 μL of NaOH (1.0 M) plus 100 μL of DMT (0.2 μM), or plus 100 μL of other substances (1.0 μM), or plus 100 μL of H_2O (control). In the UV–vis spectra of our sensors incubated with other substances, the UV–vis spectrum at visible region is very weak because the AuNPs aggregated severely due to the low electrostatic repulsion at high ionic strength, which is very similar to that of the control sample. In addition, the color our sensors incubated with other substances is grey, which is also very similar to that of the control sample. However, after incubation of the mixture of NaOH and DMT, the sensor color remains red and the UV–vis spectrum at visible region exhibited an obvious increase. These results indicate that these potential environmental pollutants have no interference to DMT detection using our AuNP-based colorimetric sensor.

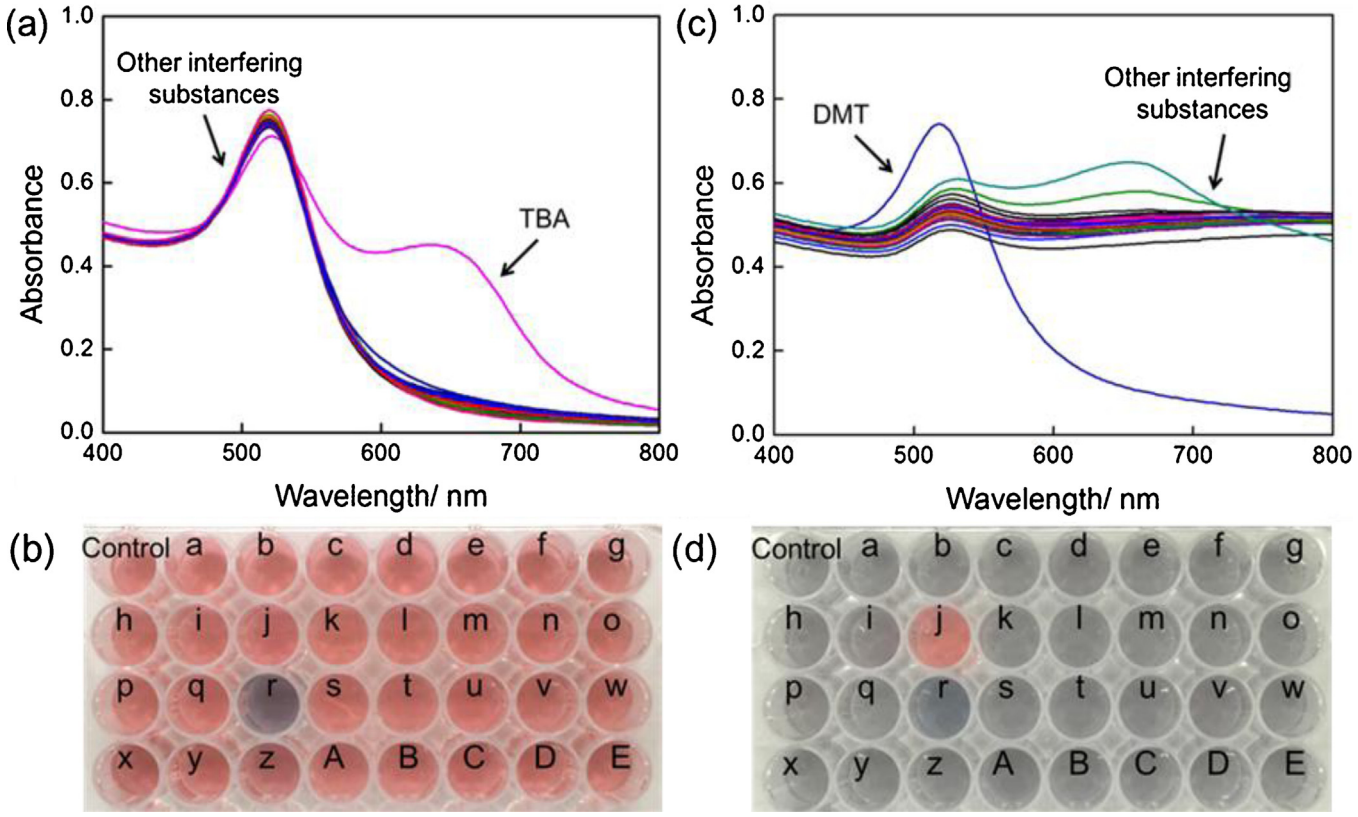

Fig. 3. Selectivity of the AuNP-based colorimetric sensor for rapid detection of TBA and DMT compared with other substances. UV–vis absorption spectra (a) and photographic images (b) of the AuNP-based colorimetric sensor (0.88 mL) incubated (5 min) with 20 μL of NaOH (1.0 M) plus 100 μL of TBA (1.0 μM), or plus 100 μL of other substances (5.0 μM), or plus 100 μL of H_2O (control); UV–vis absorption spectra (c) and photographic images (d) of the AuNP-based colorimetric sensor (0.86 mL) incubated (10 min) with 40 μL of NaOH (1.0 M) plus 100 μL of DMT(0.2 μM), or plus 100 μL of other substances (1.0 μM), or plus 100 μL of H_2O (control). a: Iprodione; b: Dioxacarb; c: Benzex; d: Isoprocarb; e: Chipton; f: Pretilachlor; g: Sodium cyclamate; h: Permethrin; i: Trichlorphon; j: Dimethoate; k: Fenvalerate; l: Chlorpyrifos; m: Profenofos; n: Indoxacarb; o: Dichlorodiphenyltrichloroethane; p: Glufosinate-ammonium; q: Glyphosate; r: Terbuthylazine; s: Deltamethrin; t: D-glucose; u: Aspartame; v: K^+; w: Na^+; x: Mg^{2+}; y: Ba^{2+}; z: Cl^-; A: NO_3^-; B: Ac^-; C: CO_3^{2-}; D: SO_4^{2-}; E: PO_4^{3-}.

3.5. Sensitivity of the AuNP-based colorimetric sensor for TBA or DMT

Under the above-mentioned optimized experimental conditions, the colorimetry observation and UV–vis spectrometry are used to evaluate the sensitivity of our AuNP-based colorimetric sensor for rapid pesticide residue detection of TBA or DMT. The photographic image of our sensors incubated with various concentration of TBA or DMT is respectively shown in Fig. 4a and d. We can see the color of the sensor gradually changes from wine red to blue with increasing of TBA concentration from 0.2 to 1.0 μM. The limit of detection (LOD) of TBA by the naked eyes is 0.3 μM, which is close to the MRL of TBA regulated by the governments of EU and China (0.22 μM) [10–12]. In addition, the color of the sensor gradually changes from grey to red with increasing of the DMT concentration from 6 to 400 nM, the LOD of DMT by eye vision is observed to be 20 nM, which is significantly lower than the MRL of DMT regulated by the governments of EU and China (87 nM) [10–12].

Fig. 4b shows the UV–vis absorption spectra of our sensors incubated with various concentrations of TBA (0.1 5.0 μM). With increasing of TBA concentration from 0.1 to 5.0 μM, the SPR band emerged with a red shift, the absorption peak at 520 nm gradually decreases, and the absorption peak at 650 nm increases gradually, which indicates that more and more AuNPs aggregate. Therefore, the variation of absorption peak intensity of AuNPs could be employed in the quantitative analysis of TBA.

In addition, Fig. 4c shows plot of A_{650}/A_{520} as a function of TBA concentration ranging from 0.1 to 5.0 μM. A_{650} and A_{520} are respectively the absorbance of 650 and 520 nm in the UV–vis spectrum of each sensor with addition of TBA. The inset of Fig. 4c shows a good linear relationship ($R^2 = 0.997$) between A_{650}/A_{520} and TBA concentrations in the range of 0.1 0.9 μM. This result demonstrates that our AuNP-based colorimetric sensor can be used for the quantitative analysis of TBA in the range of 0.1 0.9 μM. The results suggest that this probe can be used to detect TBA with a theoretical detection limit of 0.02 μM when a signal-to-noise ratio is $3(3\sigma/S)$, which is not only obviously lower than the MRL of TBA regulated by the governments of EU and China (0.22 μM), but also much lower than the LOD values of other reported TBA probes based on metal nanomaterials (Table S2) [10–12].

Fig. 4e shows the UV–vis absorption spectra of our sensors incubated with various concentrations of DMT (1 5000 nM). With increasing of DMT concentration from 1 to 5000 nM, the absorption peak at 525 nm increases gradually, which indicates that less and less AuNPs aggregate. Moreover, Fig. 4f shows plot of A_{525}/A_{680} versus DMT concentrations ranging from 1 to 5000 nM. A_{525} and A_{680} are respectively the absorbance of 525 and 680 nm in the UV–vis spectrum of each sensor with addition of DMT. The inset of Fig. 4f shows a plot of A_{525}/A_{680} versus DMT concentration ranging from 1 to 40 nM. A good linear relationship ($R^2 = 0.994$) is found between A_{525}/A_{680} and DMT concentrations. This result indicates that our AuNP-based colorimetric sensor can be used for the quantitative analysis of DMT in the range of 1 40 nM, and the LOD of DMT calculated by $3\sigma/S$ method is 6.2 nM. It's not only much lower than the MRL of DMT regulated by the governments of EU and China (87 nM) [10–12], but also much lower than the LOD values of other

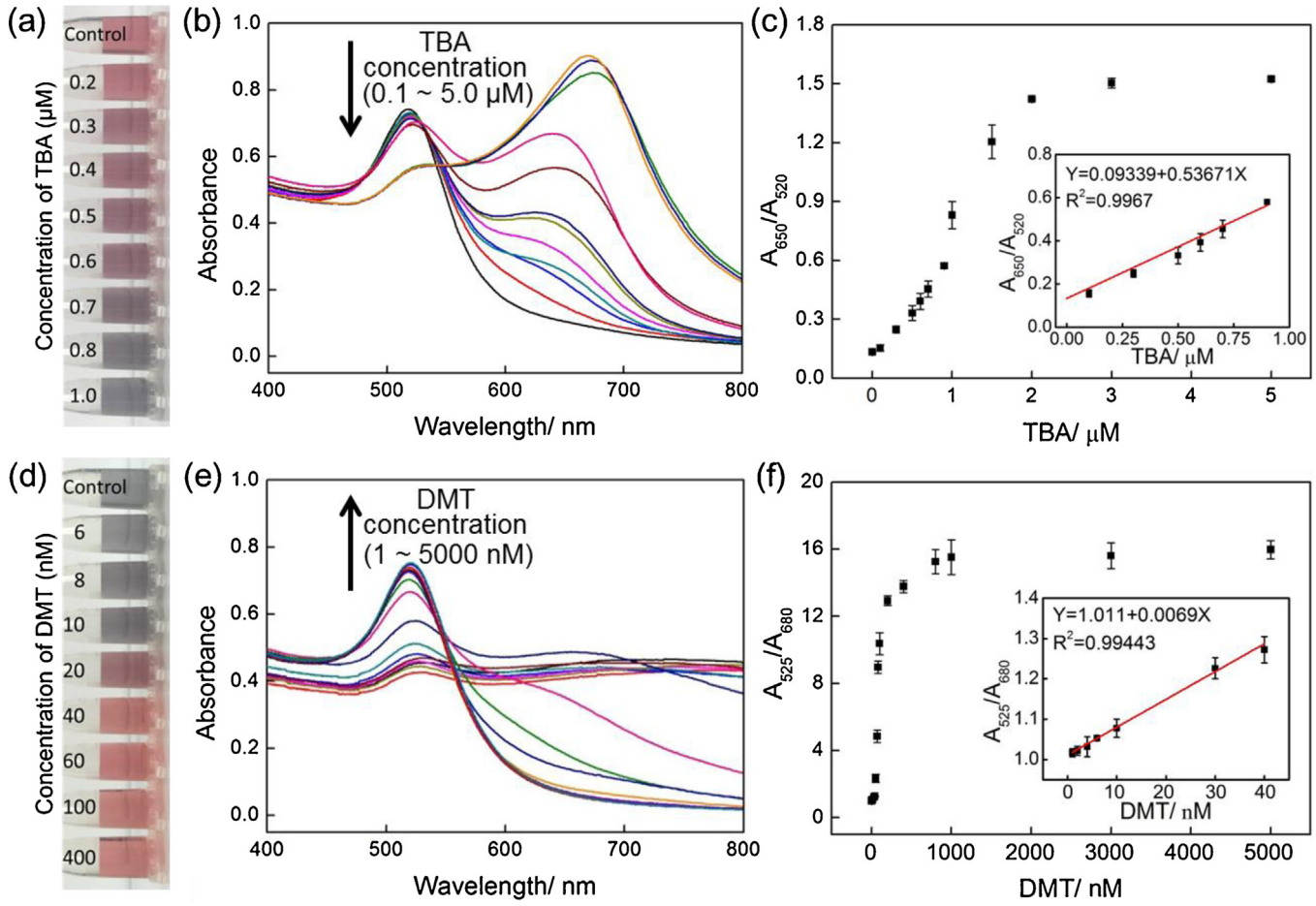

Fig. 4. Sensitivity of the AuNP-based colorimetric sensor for rapid detection of TBA and DMT. Photographic images (a) and UV–vis absorption spectra (b) of the AuNP-based colorimetric sensors (0.88 mL) incubated (5 min) with 20 μL of NaOH (1.0 M) plus 100 μL of TBA, or plus 100 μL of H_2O (control). The TBA concentration range is 0.2 1.0 μM for the colorimetry observation, but 0.1 5.0 μM for the UV–vis spectrometry. (c): Plot of A_{650}/A_{520} as a function of the TBA concentrations ranging from 0.1 to 5.0 μM. Photographic images (d) and UV–vis absorption spectra (e) of the AuNP-based colorimetric sensors (0.86 mL) incubated (10 min) with 40 μL of NaOH (1.0 M) plus 100 μL of DMT, or plus 100 μL of H_2O (control). The DMT concentration range is 6 400 nM for the colorimetry observation, but 1 5000 nM for the UV–vis spectrometry. (f): Plot of A_{525}/A_{680} as a function of the DMT concentrations in the range of 1–5000 nM.

reported DMT probes based on noble metal nanomaterials (Table S2) [26–28,38–40].

3.6. Detection of TBA or DMT in real environmental samples

To evaluate the practical applicability, our AuNP-based colorimetric sensor is further applied for TBA or DMT detection in real environmental samples (i.e. tap water, green tea or apple juice). Because the real environmental samples have no TBA or DMT contamination, they were spiked with standard solutions of TBA (0.1–2.5 μM) or DMT (10–500 nM). Fig. 5 shows the rapid colorimetric detection of TBA or DMT with various concentrations in the real liquid samples. In the group of TBA detection (Fig. 5a), the color of the control samples is red, and the color of the sensors with various concentrations of TBA gradually changes from red to blue. The LOD of TBA detection in the tap water, green tea or apple juice are respectively observed to be 0.2, 0.4 and 0.1 μM because of the visible color difference between the sensors with TBA and control sample. Furthermore, in the group of DMT detection (Fig. 5b), the color of the control samples is grey or grey red, and the color of the sensors with various DMT concentrations gradually changes to bright red. The LOD of DMT detection in the tap water, green tea or apple juice are respectively observed to be 100, 50 and 100 nM due to the obvious color difference between the sensors with DMT and control sample. Similar LOD values of TBA or DMT in these real environmental samples are also observed by the UV–vis spectrometry (Fig. S6). These results demonstrate that our AuNP-based colorimetric sensor has a good practical applicability for TBA or DMT detection in the real environmental samples.

Our AuNP-based colorimetric sensor can be used for detection of TBA or DMT, but cannot be used for the detection of an environmental sample that could contain both TBA and DMT. That's because both detections are based on different mechanisms, and both detection protocols are also different. TBA detection is based on aggregation mechanism, and 20 μL of NaOH (1.0 M) should be added into 100 μL of sample before mixing with our sensor. However, DMT detection is based on anti-aggregation mechanism, and 40 μL of NaOH (1.0 M) should be added into 100 μL of sample before mixing with our sensor.

4. Conclusions

In this study, we developed a new colorimetric sensor based on citrate-stabilized AuNPs for the rapid pesticide residue detection of both TBA and DMT with ultra-sensitivities and high selectivities. The TBA detection is based on an aggregation mechanism, and the DMT detection is based on an anti-aggregation mechanism. These mechanisms have been verified via FT-IR, UV–vis spectra, Zeta Potential, TEM and DLS. Under the optimized experimental conditions, 30 kinds of potential environmental pollutants have no

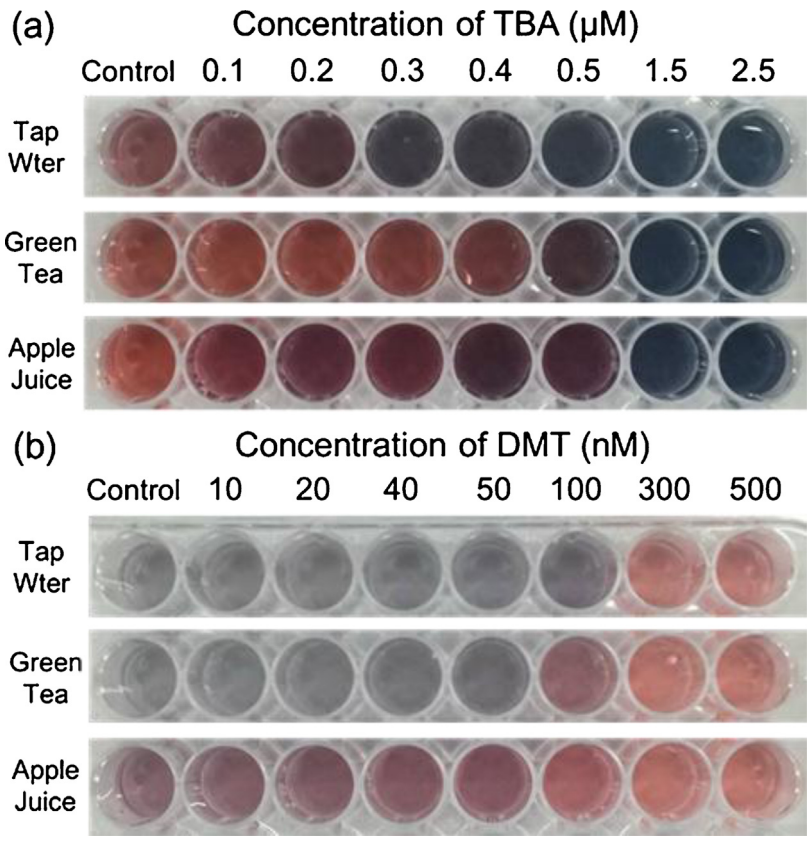

Fig. 5. Rapid colorimetric detection of TBA (a) and DMT (b) with various concentrations in real environmental samples. (a): 0.88 mL of the AuNP-based colorimetric sensors incubated (5 min) with 20 μL of NaOH (1.0 M) plus 100 μL of TBA (0.1 2.5 μM) in real liquid samples; (b): 0.86 mL of the AuNP-based colorimetric sensors incubated (10 min) with 40 μL of NaOH (1.0 M) plus 100 μL of DMT (10 500 nM) in real liquid samples. The real liquid samples without TBA and DMT are used instead of that with TBA or DMT as the controls.

interference on the TBA or DMT detection indicating the high selectivities of our AuNP-based colorimetric sensor. The LOD of TBA is 0.3 μM by the naked eyes, and 0.02 μM by calculation (3σ/S), which is obviously lower than the MRL of TBA regulated by the governments of EU and China (0.22 μM). The LOD of DMT is 20 nM by eye vision, and 6.2 nM by calculation (3σ/S), which are both much lower than the MRL of DMT regulated by the governments of EU and China (87 nM). These low LODs indicate the ultra-sensitivities of our AuNP-based colorimetric sensor. The linear relationships of the UV–vis spectrometry demonstrate that our AuNP-based colorimetric sensor can be used for the quantitative analysis of TBA in the range of 0.1 0.9 μM, and DMT in the range of 1–40 nM. Finally, our AuNP-based colorimetric sensor is also verified to have a good practical applicability for TBA or DMT detection in the real environmental samples.

Acknowledgments

This work is financially supported by the Project for Science and Technology Service of Chinese Academy of Sciences (KFJ-SW-STS-172), National Key Research & Development Program (2016YFC1400600), Youth Innovation Promotion Association of Chinese Academy of Sciences (2016269), Hundred Talents Program of Chinese Academy of Sciences (2010-735), Public Welfare Technology Application Research Project of Zhejiang Province (2017C33129), Zhejiang Provincial Natural Science Foundation of China (Grant No. R5110230), National Natural Science Foundation of China (Grant Nos. 61571278, 81401452 and 21305148), the aided program for Science and Technology Innovative Research Team of Ningbo Municipality (Grant No. 2015B11002).

Appendix A. Supplementary data

Supplementary data associated with this article can be found, in the online version, at https://doi.org/10.1016/j.snb.2017.09.134.

References

[1] M. Pateiromoure, M. Ariasestévez, J. Simalgándara, Critical review on the environmental fate of quaternary ammonium herbicides in soils devoted to vineyards, Environ. Sci. Technol. 47 (2013) 4984–4998.
[2] X. Wang, X.J. Li, Z. Li, Y.D. Zhang, Y. Bai, H.W. Liu, Online coupling of in-tube solid-phase microextraction with direct analysis in real time mass spectrometry for rapid determination of triazine herbicides in water using carbon-nanotubes-incorporated polymer monolith, Anal. Chem. 86 (2014) 4739–4747.
[3] D. Jiang, X.J. Du, Q. Liu, L. Zhou, J. Qian, K. Wang, One-step thermal-treatment route to fabricate well-dispersed ZnO nanocrystals on nitrogen-doped graphene for enhanced electrochemiluminescence and ultrasensitive detection of pentachlorophenol, ACS Appl. Mater. Interfaces 7 (2015) 3093–3100.
[4] I. Gardi, S. Nir, Y.G. Mishael, Filtration of triazine herbicides by polymer-clay sorbents: coupling an experimental mechanistic approach with empirical modeling, Water Res. 70 (2015) 64–73.
[5] H.V. Lutze, S. Bircher, I. Rapp, N. Kerlin, R. Bakkour, M. Geisler, C.V. Sonntag, T.C. Schmidt, Degradation of chlorotriazine pesticides by sulfate radicals and the influence of organic matter, Environ. Sci. Technol. 49 (2015) 1673–1680.
[6] D.N. Priya, J.M. Modak, P. Trebse, R. Zabar, A.M. Raichur, Photocatalytic degradation of dimethoate using LbL fabricated TiO_2/polymer hybrid films, J. Hazard. Mater. 195 (2011) 214–222.
[7] P. Caregnato, J.A. Rosso, J.M. Soler, A. Arques, D.O. Martire, M.C. Gonzalez, Chloride anion effect on the advanced oxidation processes of methidathion and dimethoate: role of Cl-2(center dot-) radical, Water Res. 47 (2013) 351–362.
[8] J. Karpeta-Kaczmarek, M. Kubok, M. Dziewiecka, T. Sawczyn, M. Augustyniak, The level of DNA damage in adult grasshoppers Chorthippus biguttulus (Orthoptera, Acrididae) following dimethoate exposure is dependent on the insects' habitat, Environ. Pollut. 215 (2016) 266–272.

[9] P.M. Alvarez, D.H. Quinones, I. Terrones, A. Rey, F.J. Beltran, Insights into the removal of terbuthylazine from aqueous solution by several treatment methods, Water Res. 98 (2016) 334–343.
[10] Council Directive 98/83/EC on the Quality of Water Intended For Human Consumption, European Community, 2015.
[11] The commission of the european communities: commission regulation (EC) No 149/2008, Off. J. Eur. Union (2008) 1–398.
[12] U. Hoffmann, T. Papendorf, Organophosphate poisonings with parathion and dimethoate, Intensive Care Med. 32 (2006) 464–468.
[13] F. Hernandez, T. Portoles, E. Pitarch, F.J. Lopez, Target and nontarget screening of organic micropollutants in water by solid-phase microextraction combined with gas chromatography/high-resolution time-of-flight mass spectrometry, Anal. Chem. 79 (2007) 9494–9504.
[14] A. Salemi, R. Rasoolzadeh, M.M. Nejad, M. Vosough, Ultrasonic assisted headspace single drop micro-extraction and gas chromatography with nitrogen-phosphorus detector for determination of organophosphorus pesticides in soil, Anal. Chim. Acta 769 (2013) 121–126.
[15] W.J. Zhao, X.K. Sun, X.N. Deng, L. Huang, M.M. Yang, Z.M. Zhou, Cloud point extraction coupled with ultrasonic-assisted back-extraction for the determination of organophosphorus pesticides in concentrated fruit juice by gas chromatography with flame photometric detection, Food Chem. 127 (2011) 683–688.
[16] B.A. Khan, A. Farid, M.R. Asi, H. Shah, A.K. Badshah, Determination of residues of trichlorfon and dimethoate on guava using HPLC, Food Chem. 114 (2009) 286–288.
[17] R.X. Mou, M.X. Chen, Z.Y. Cao, Z.W. Zhu, Simultaneous determination of triazine herbicides in rice by high-performance liquid chromatography coupled with high resolution and high mass accuracy hybrid linear ion trap-orbitrap mass spectrometry, Anal. Chim. Acta 706 (2011) 149–156.
[18] C.J. Choi, J.A. Berges, E.B. Young, Rapid effects of diverse toxic water pollutants on chlorophyll a fluorescence: variable responses among freshwater microalgae, Water Res. 46 (2012) 2615–2626.
[19] Q. Long, H.T. Li, Y.Y. Zhang, S.Z. Yao, Upconversion nanoparticle-based fluorescence resonance energy transfer assay for organophosphorus pesticides, Biosens. Bioelectron. 68 (2015) 168–174.
[20] L. Mosiello, C. Laconi, M. Del Gallo, C. Ercole, A. Lepidi, Development of a monoclonal antibody based potentiometric biosensor for terbuthylazine detection, Sens. Actuator B-Chem. 95 (2003) 315–320.
[21] S.H. Li, J.H. Luo, G.H. Yin, Z. Xu, Y. Le, X.F. Wu, N.C. Wu, Q. Zhang, Selective determination of dimethoate via fluorescence resonance energy transfer between carbon dots and a dye-doped molecularly imprinted polymer, Sens. Actuator B-Chem. 206 (2015) 14–21.
[22] P. Venkateswarlu, K.R. Mohan, C.R. Kumar, K. Seshaiah, Monitoring of multi-class pesticide residues in fresh grape samples using liquid chromatography with electrospray tandem mass spectrometry, Food Chem. 105 (2007) 1760–1766.
[23] J.V. Rohit, H. Basu, R.K. Singhal, S.K. Kailasa, Development of p-nitroaniline dithiocarbamate capped gold nanoparticles-based microvolume UV–vis spectrometric method for facile and selective detection of quinalphos insecticide in environmental samples, Sens. Actuator B-Chem. 237 (2016) 826–835.
[24] R. Bala, M. Kumar, K. Bansal, R.K. Sharma, N. Wangoo, Ultrasensitive aptamer biosensor for malathion detection based on cationic polymer and gold nanoparticles, Biosens. Bioelectron. 85 (2016) 445–449.
[25] Y.Q. Chang, Z. Zhang, J.H. Hao, W.S. Yang, J.L. Tang, A simple label free colorimetric method for glyphosate detection based on the inhibition of peroxidase-like activity of Cu(II), Sens. Actuator B-Chem. 228 (2016) 410–415.
[26] Q.L. Lang, L. Han, C.T. Hou, F. Wang, A.H. Liu, A sensitive acetylcholinesterase biosensor based on gold nanorods modified electrode for detection of organophosphate pesticide, Talanta 156 (2016) 34–41.
[27] A.I. Dar, S. Walia, A. Acharya, Citric acid-coated gold nanoparticles for visual colorimetric recognition of pesticide dimethoate, J. Nanopart. Res. 18 (2016), http://dx.doi.org/10.1007/s11051-016-3553-4.
[28] S.K. Menon, N.R. Modi, A. Pandya, A. Lodha, Ultrasensitive and specific detection of dimethoate using a p-sulphonato-calix[4] resorcinarene functionalized silver nanoprobe in aqueous solution, RSC Adv. 3 (2013) 10623–10627.
[29] Y.Z. Xia, X.X. Wu, J.T. Zhao, J.S. Zhao, Z.H. Li, W.Z. Ren, Y.C. Tian, A.G. Li, Z.Y. Shen, A.G. Wu, Three dimensional plasmonic assemblies of AuNPs with an overall size of sub-200 nm for chemo-photothermal synergistic therapy of breast cancer, Nanoscale 8 (2016) 18682–18692.
[30] X.X. Wu, L.Q. Luo, S.G. Yang, X.H. Ma, Y.L. Li, C. Dong, Y.C. Tian, L.E. Zhang, Z.Y. Shen, A.G. Wu, Improved SERS nanoparticles for direct detection of circulating tumor cells in the blood, ACS Appl. Mater. Interfaces 7 (2015) 9965–9971.
[31] Y.L. Li, Y.M. Leng, Y.J. Zhang, T.H. Li, Z.Y. Shen, A.G. Wu, A new simple and reliable Hg^{2+} detection system based on anti-aggregation of unmodified gold nanoparticles in the presence of *O*-phenylenediamine, Sens. Actuator B-Chem. 200 (2014) 140–146.
[32] C. Carrillo-Carrion, B.M. Simonet, M. Valcarcel, B. Lendl, Determination of pesticides by capillary chromatography and SERS detection using a novel Silver-Quantum dots sponge nanocomposite, J. Chromatogr. A 1225 (2012) 55–61.
[33] Y. Ma, L.Y.L. Yung, Detection of dissolved CO_2 based on the aggregation of gold nanoparticles, Anal. Chem. 86 (2014) 2429–2435.
[34] J.Y. Kang, Y.J. Zhang, X. Li, L.J. Miao, A.G. Wu, A Rapid Colorimetric sensor of clenbuterol based on cysteamine-modified gold nanoparticles, ACS Appl. Mater. Interfaces 8 (2016) 1–5.
[35] J.J. Yao, M.R. Hoffmann, N.Y. Gao, Z. Zhang, L. Li, Sonolytic degradation of dimethoate: kinetics, mechanisms and toxic intermediates controlling, Water Res. 45 (2011) 5886–5894.
[36] J.Q. Chen, D. Wang, M.X. Zhu, C.J. Gao, Photocatalytic degradation of dimethoate using nanosized TiO_2 powder, Desalination 207 (2007) 87–94.
[37] M. Catala-Icardo, J.L. Lopez-Paz, C. Choves-Baron, A. Pena-Badena, Native vs photoinduced chemiluminescence in dimethoate determination, Anal. Chim. Acta 710 (2012) 81–87.
[38] C.W. Hsu, Z.Y. Lin, T.Y. Chan, T.C. Chiu, C.C. Hu, Oxidized multiwalled carbon nanotubes decorated with silver nanoparticles for fluorometric detection of dimethoate, Food Chem. 224 (2017) 353–358.
[39] R.P. Liang, X.N. Wang, C.M. Liu, X.Y. Meng, J.D. Qiu, Construction of graphene oxide magnetic nanocomposites-based on-chip enzymatic microreactor for ultrasensitive pesticide detection, J. Chromatogr. A 1315 (2013) 28–35.
[40] S.L. Wang, X.B. Wang, X.X. Chen, X.Z. Cao, J. Cao, X.F. Xiong, W.B. Zeng, A novel upconversion luminescence turn-on nanosensor for ratiometric detection of organophosphorus pesticides, RSC Adv. 6 (2016) 46317–46324.

Biographies

Ning-Yi Chen received her master degree from University of Science and Technology of China in 2016. She has been receiving united training in Ningbo Institute of Materials Technology and Engineering, Chinese Academy of Sciences since 2014. Chen's research focused on the preparation of the precious metal nanoparticles and approach for the detection of heavy metal ions or organic pesticides.

Hong-Yu Liu received his master degree from University of Science and Technology of China in 2016. He has been receiving united training in Ningbo Institute of Materials Technology and Engineering, Chinese Academy of Sciences since 2014. His current research focuses on the chemical method for heavy metal pollution remediation.

Yu-Jie Zhang is an associate professor in Ningbo Institute of Materials Technology and Engineering, Chinese Academy of Sciences from 2011 and engages in the detection of metal ions based on AuNPs study.

Zhuang-Wei Zhou is studying for a master's degree in Ningbo University and also receiving united training in Ningbo Institute of Materials Technology & Engineering, Chinese Academy of Sciences, working under the supervision of Prof. Aiguo Wu. His research interests are detection of organic pesticides based on precious metal nanoparticles.

Wen-Pei Fan received his PhD in 2015 from Shanghai Institute of Ceramics, Chinese Academy of Sciences (SICCAS) under the direction of Prof. Wenbo Bu and Prof. Jianlin Shi. He then worked with Prof. Xiaoyuan (Shawn) Chen at National Institutes of Health (NIH) as a postdoctoral fellow in 2015. His research interest focuses on the design and synthesis of multifunctional nanotheranostics for multimodal imaging guided synergistic therapy.

Guo-Can Yu received his PhD in Chemistry from the Zhejiang University in 2015 under the mentorship of Prof. Feihe Huang. Then he joined Dr Xiaoyuan (Shawn) Chen's Laboratory of Molecular Imaging and Nanomedicine (LOMIN) at the National Institute of Biomedical Imaging and Bioengineering (NIBIB), National Institutes of Health (NIH), as a postdoctoral research fellow. His current research interests are focused on supramolecular chemistry, supramolecular hybrid materials and supramolecular theranostics.

Zhen-Yu Shen is a visiting scholar of National Institutes of Health (USA) under supervision of Prof. Xiaoyuan Chen. He earned his PhD from Institute of Process Engineering, Chinese Academy of Sciences, under supervision of Prof. Guanghui Ma and Prof. Toshiaki Dobashi (Gunma University, Japan). After postdoctoral studies with Prof. Kazuhiro Kohama (Gunma University, Japan) and Prof. Sheng Dai (The University of Adelaide, Australia), he was appointed an Associate Professor (2012) and promoted to Full Professor (2015) at Ningbo Institute of Materials Technology & Engineering, Chinese Academy of Sciences. His research interests include: environmental pollutants' detection, noble metal nanoparticles, circulating tumor cells, surface-enhanced Raman scattering, and molecular imaging.

Ai-Guo Wu has been a professor and postgraduate student tutor in Ningbo Institute of Materials Technology and Engineering, Chinese Academy of Sciences since 2009 and engages in the applications of various nanomaterials in biomedicine, bioanaytical chemistry and environmental sciences. He earned his PhD from Changchun Institute of Applied Chemistry, Chinese Academy of Sciences, under supervision of Prof. Erkang Wang and Prof. Zhuang Li. After postdoctoral studies with Prof. Norbert A. Hampp (University of Marburg, Germany) and Prof. Ahmed H. Zewail (Nobel Laureate for Chemistry in 1999, California Institute of Technology, USA), then he moved to Feinberg School of Medicine, Northwestern University in USA. He was appointed Full Professor (2009) at Ningbo Institute of Materials Technology & Engineering, Chinese Academy of Science.